A Distributed Hierarchical Control Framework in Islanded Microgrids and Its Agent-Based Design for Cyber-Physical Implementations

Tung-Lam Nguyen, Yu Wang, Quoc-Tuan Tran, Raphael Caire, Yan Xu, Catalin Gavriluta

A Distributed Hierarchical Control Framework in Islanded Microgrids and Its Agent-based Design for Cyber-Physical Implementations

Tung-Lam Nguyen, Yu Wang, *Member, IEEE*, Quoc-Tuan Tran, *Senior Member, IEEE,* Raphael Caire, *Senior Member, IEEE,* Yan Xu, *Senior Member, IEEE,* Catalin Gavriluta

***Abstract*—In this paper, a distributed hierarchical control framework with coordinated secondary and tertiary levels is proposed for islanded microgrids (MGs). The structure and functionality of each agent are formulated to process simultaneously the secondary control and tertiary control in a peer-to-peer communication network. First, the distributed secondary control is proposed for restoring system frequency/voltage while providing power sharing considering droop coefficients and upper level power dispatch orders. Then the distributed tertiary control minimizes the network power loss in the islanded MG by using alternating direction method of multipliers (ADMM) algorithm. The multi-agent system is designed to cover both control levels for cyber-physical implementations. A laboratory cyber-physical MG platform has been built to validate the proposed control framework in real-time and hardware-in-the-loop conditions. A six-bus three-DG MG is implemented on the platform and the experimental results validate the effectiveness of the proposed method.**

***Index Terms*—distributed control, hierarchical control, ADMM, hardware-in-the-loop, multi-agent system.**

I. Introduction

MICROGRIDS (MGs), as fundamental subsystems in future power system, are integrated with distributed generators (DGs), controllable and non-controllable loads, energy storage systems (ESSs), as well as sophisticated control and communication systems [1], [2]. The MG consists of both electrical and communication infrastructure that forms a complex cyber-physical system. The control system based on communication and sensor network is becoming a major topic to be investigated in the future cyber-physical MG.

The operation of DGs plays a crucial role to guarantee the stability and reliability of MGs, especially in the islanded mode. Nevertheless, the central controller of MGs with a large amount of DGs may face to challenges of large communication and computation burdens, single point failure, data privacy, etc. Managing MGs with the increasing integration of controllable entities requires new scalable control strategies, that are robust to the cyber and physical network disturbances. The distributed control strategies have attracted much attention which provides the same control objectives as the centralized one and offers greater scalability, reliability, and resiliency [3].

T.L. Nguyen was with Univ. Grenoble Alpes, G2Elab, F-38000 Grenoble, France and is currently with The University of Danang – University of Science and Technology, Danang, Vietnam (ntlam@dut.udn.vn).

Y. Wang and Y. Xu are with Nanyang Technological University, Singapore 639798 (e-mail:wang_yu@ntu.edu.sg). (Corresponding author: Yu Wang)

Q.T. Tran is with Univ. Grenoble Alpes, CEA, LITEN, INES, Department of Solar Technologies, F-73375 Le Bourget du Lac, France.

R. Caire is with Univ. Grenoble Alpes, G2Elab, F-38000 Grenoble, France.

C. Gavriluta is with AIT Austrian Institute of Technology, Austria.

Nowadays, the existing control systems of MGs is developed in a hierarchical way [4]. The hierarchies of MG control are divided into three levels, i.e. primary control (PC), secondary control (SC) and tertiary control (TC) with different time-scales and objectives. The PC usually refers to the local control of DGs, which is to achieve fast and stable power tracking and autonomous power sharing. The SC aims to restore rated conditions of the system and achieve voltage/frequency restoration, accurate power sharing, etc. The TC is at the top level which realizes the global optimal operation of MGs. Recently, many works have been reported on the contributions of distributed strategies in a range of MGs applications. Nonetheless, these works mostly focus on one control level (SC or TC) instead of including PC, SC or TC into a single control framework.

Systematic surveys of the SC techniques of MGs are presented in [3], [5]. The works in [6] proposes a distributed averaging-based control structure that one DG averages the values received from neighbors to build control signals. Later on, various improved methods are proposed for distributed SC of microgrids, including non-linear [7], model predictive control [8], optimal control [9], etc. The event-triggered control has been employed to reduce the amount of communication exchanged among DGs while maintaining system stability [10], [11]. The main functions of SC include frequency/voltage restoration, state of charge balancing, harmonic mitigation, etc. The power outputs of DGs are shared proportionally following droop coefficients. Several works have considered the generation cost for the economic dispatch purpose [12], but they ignore power flow constraints. With only SC, the global optimal operation of the MG, therefore, can not be achieved.

On the other hand, methods of distributed TC, or distributed optimal power flow (OPF) process, are thoroughly investigated in [13], [14]. ADMM, which based on augmented Lagrangian decomposition, is widely used to solve OPF problems because the convergence is improved [15], [16]. Recently augmented Lagrangian alternating direction inexact Newton (ALADIN) method has been developed to solve non-convex OPF problem with the consensus results are converged in less number of iterations compared with ADMM [17]. Research concerning distributed OPF, however, only consider mathematical formulations and show numerical results without validation in dynamic environment regarding disturbances of the system. Moreover, in these works, the frequency and voltage control are ignored due to the fact that there is a slack bus in studied grids which always stabilizes the system and maintains frequency/voltage at rated values. In islanded mode, MG is

usually governed by a set of droop controlled DGs in parallel. The OPF process in this case therefore has to coordinate with lower control (PC and SC) to guarantee the optimal operation as well as the nominal state of frequency/voltage.

The distributed SC and TC objectives are mostly resolved independently since they work for distinguish aims and happen in separated timescales. In the literature, only several works have been conducted for both SC and TC in a single control framework of MGs. The works in [18], [19] have introduced cooperative control modules to achieve hierarchical goals, however, in the TC level, the modules aim to solve economic dispatch problem without power flow constraints. In [20], authors have presented a fully distributed hierarchical control for islanded MGs. Although implementing test case simulation in the time domain, this research ignores the time consumed by the optimization processes. Moreover, the interaction between SC and TC level is still not clarified.

The multi-agent system (MAS) is a technique widely used to implement distributed control methods in MGs [21], [22]. The MAS, in real-world applications, is a cluster of entities located at distinctive places. Messages are transferred between neighborhood agents through a communication network. An agent is a program running in a processor (e.g., PLC, computer) for specific purposes. Challenges on implementing MAS in cyber-physical MG system need further intensive investigation for practical deployment. Various distributed algorithms have been proposed to control and optimize the operation of AC MGs. The proposed methods can be validated via pure software simulations (the agent system is integrated into the grid simulators) or use an existing MAS platform to co-simulate with MG simulation. In these approaches, the agent system usually runs in a single process without communication network. The other plan is to conduct the test system in a pure hardware platform with all components of MGs are physical devices, so the validation is more realistic [23]. Nevertheless, the scale of MG is limited and the test case MG is hard to be expanded. Some works introduce the platform with hardware agents cooperating with a real-time simulator [24], [25]; however, there is no specific control method presented or centralized control schemes applied in these works.

In order to deploy the distributed hierarchical control in islanded MGs, the realization of MAS with two control levels is still facing challenges that have not been resolved in the literature. Firstly, the agent manages simultaneously the distributed SC and TC algorithms with distinctive timescales and objectives. The operation mechanism of agent is still needed more comprehensive studies for the coordination as well as toward practical implementation with the consideration on time-consuming of computation. Secondly, the requirements of communication network and exchanged information for distributed SC and TC are different while one agent is designed to conduct both control levels. This issue will be discussed more detail in Section III-B. Thirdly, the gap between theoretical analysis and practical deployments is still large. It is necessary to provide a practical way to operate the MAS in different processors under realistic communication with various issues e.g. latency, packet losses. The design of agents in the relationships with devices and controllers also need to be clarified for real implementations.

The major contributions of this paper are:

- A distributed hierarchical control method for islanded MGs is provided. The control system is constructed to achieve multiple functionalities: SC objectives are to remain voltage/frequency at reference values and arbitrarily sharing power, and the TC objective is to optimize the grid operation.
- The design of agents in MAS is proposed with the ability of implementing in realistic conditions. By exchanging data under a communication network, each agent is constructed to run two parallel SC and TC processes.
- We go through from the stability analysis to realistic validation with a cyber-physical system in a hardware-in-the-loop test-bed. The hardware agents, as independent entities, can operate asynchronously under a real communication network that reflects the operation of the MAS in the real world.

II. A Fully Distributed Hierarchical Control in Islanded Microgrids

In the MG control hierarchies, the key points differentiating each control level are control objectives, response speed and infrastructure requirement (e.g. communication). When a small disturbance occurs, primary control reacts immediately to provide a fast response to stabilize the system. Then the SC is activated, basically, for the restoration of frequency or voltage. The TC, as a higher and slower response control level, will try to optimize the grid operation. In the distributed hierarchical control framework, the entire operation and control of islanded MGs can be realized based on only sparse communications.

The $\mathcal{N}$ bus MG operated in islanded mode is supplied by several DGs. The set of DG buses is $\mathcal{G} \subseteq \mathcal{N}$. The coordination is mandatory because, in high control levels, the DGs concurrently contribute to regulate frequency/voltage or to redistribute power flow in grids for optimal operation. The three control levels in a fully distributed hierarchical structure will be investigated in this section.

A. Primary Control

The primary droop control is to emulate characteristics of synchronous generator which is performed by turbine governor, voltage regulator and generator inertia. In islanded AC MG, the inverter interfaced DGs are controlled as voltage source inverters. Therefore, apart from droop control, an inner control loop which consists of a current control loop and a voltage control loop is required. Besides, in order to achieve accurate power sharing among each unit, a virtual impedance loop can also be considered.

Droop control is widely used to control the magnitude of voltage and frequency in case of inverter interfaced DGs in islanded MGs. The dynamic droop characteristic for *i*th DG is shown as follows [1], [2]:

$$\omega_i = \omega^* - K_i^P P_i^m \tag{1}$$

$$V_i = V^* - K_i^Q Q_i^m \tag{2}$$

where ω^* and V^* are the nominal frequency and voltage amplitude. K_i^P and K_i^Q are droop coefficients, which are commonly chosen based on the output power rating. P_i^m and Q_i^m are the measured active and reactive power output. ω_i and V_i are then adjusted to return to nominal values by control signals sent from the SC level.

B. Distributed Secondary Control

The distributed SC is to achieve three objectives: 1) frequency restoration, 2) voltage restoration, and 3) arbitrary power sharing. Based on the developed PC, the functionalities of SC can be obtained by changing the frequency and voltage set points.

In the distributed SC scheme, each DG exchanges information with several other DGs. The connections between DGs are depicted by a graph with the set of nodes corresponding to the set of DG buses $\mathcal{G}$ and the set of edges $\mathcal{E} = \mathcal{G} \times \mathcal{G}$.

Consider the first-order low-pass filters for the active and reactive power measurement P_i^m and Q_i^m:

$$\tau_i^P \dot{P_i^m} = -P_i^m + P_i \tag{3}$$

$$\tau_i^Q \dot{Q_i^m} = -Q_i^m + Q_i \tag{4}$$

where τ_i^P and τ_i^Q are the time constant of the filters. P_i and Q_i are the active and reactive power of each DG.

Combine (3) and (4) with the droop control (1) and (2), the dynamics of MG system with control inputs is represented by:

$$\tau_i^P \dot{\omega}_i = -\omega_i + \omega^* - K_i^P P_i + u_i^\omega + u_i^P \tag{5}$$

$$\tau_i^Q \dot{V}_i = -V_i + V_i^* - K_i^Q Q_i + u_i^V \tag{6}$$

where u_i^ω, u_i^P and u_i^V are the control inputs of the system.

Based on the ideas of consensus control, the differences of frequency and voltage between two adjacent DGs will be eliminated. The frequency and voltage will be restored to their nominal values ω^* and V^*. The secondary frequency and voltage control laws can be designed as follows [6], [26]:

$$\dot{u}_i^\omega = c_1[\sum_{j=1}^{N} a_{ij}(\omega_j - \omega_i) + g_i(\omega^* - \omega_i)] \tag{7}$$

$$\dot{u}_i^V = c_2[\sum_{j=1}^{N} a_{ij}(V_j - V_i) + g_i(V^* - V_i)] \tag{8}$$

In addition, the arbitrary power sharing among all DGs while considering TC inputs are achieved by:

$$\dot{u}_i^P = \quad c_3 \sum_{j=1}^{N} a_{ij}[K_j^P(P_j - P_j^{Ter}) - K_i^P(P_i - P_i^{Ter})] \tag{9}$$

where P_i^{Ter} and P_j^{Ter} are control signals from the TC level; c_1, c_2, c_3 are control gains; a_{ij} is the communication coefficient between DGs *i* and *j*, $a_{ij} = 1$ if $(i,j) \in \mathcal{E}$, otherwise, $a_{ij} = 0$; g_i is the pinning gain of the DG *i*, $g_i = 1$ if the DG can directly receive the set points information, and $g_i = 0$ otherwise.

Remark 1: As discussed in [27], the coefficients a_{ij} is the elements in adjacent matrix A. To ensure the convergence of consensus algorithms, the communication graph described by matrix A should be a connected graph. For the undirected graph considered in this paper, all the nodes in the graph should be connected by edges. These are the constraints which should be satisfied by the proposed controllers in (7)-(9). Let L be the Laplacian matrix of the communication graph. The second smallest eigenvalue of L influences the convergence speed. Besides, the convergence speed of the proposed control can be adjusted by c_1, c_2, c_3. It is noted that there is a trade-off relationship between convergence speed and tolerance to communication delays [27].

C. Distributed Tertiary Control

The distributed TC is aimed to optimize the operation of the microgrid. In this work, the objective is to minimize the total network power losses. The control in this level is the OPF process of solving the OPF problem. Since the dynamics of frequency and voltage restoration are much faster, the values of frequency and voltage in the TC process can be considered at steady-states. Thus the buses with DGs when formulating the problem can be mentioned as *PV buses* where voltages are kept at a reference value and the active power values P are determined by the solution of the OPF problem. The buses with only loads are considered as *PQ buses*. The TC will compute the active power references for lower control levels, which is P^{Ter} in (9). The power outputs of DG units will pursue the references to make the system achieve the optimal state. The ADMM is implemented to solve the OPF problem in a distributed way.

In the distributed TC, the communication graph for information exchange is identical to the grid network. Nodes of the graph are the set of all buses $\mathcal{N}$. Edges of the graph are identified from the power lines of the power system.

1) ADMM: Alternating Direction Method of Multipliers algorithm is for solving a distributed optimization problem [28]. The main advantage of using ADMM is that it inherits the benefits of dual decomposition and augmented Lagrangian methods for constrained optimizations. We now consider the problem in a general form consensus optimization with the objective and constraint terms can be split into K parts:

$$\begin{aligned} \text{minimize} \quad & \sum_{k=1}^{K} f_k(\mathbf{x}_k) \\ \text{subject to} \quad & \mathbf{x}_k - \tilde{\mathbf{z}}_k = 0, \quad k = 1, 2, \ldots, K \end{aligned} \tag{10}$$

where $\mathbf{x}_k \in \mathbb{R}^{N_k}$ is the local variable, $\mathbf{z} \in \mathbb{R}^N$ is the global variable, $\tilde{\mathbf{z}} \in \mathbb{R}^{N_k}$ is the fraction of the global variable $\mathbf{z}$ that local variable $\mathbf{x}_k$ should be.

According to [28], without loss of generalization, we can insert additional constraints in the local variables $\mathbf{x}_k$ to (10).

The augmented Lagrangian for the problem (10) is:

$$L_\rho(\mathbf{x}, \mathbf{z}, \lambda) = \sum_{k=1}^{K} (f_k(\mathbf{x}_k) + \boldsymbol{\lambda}_k^T(\mathbf{x} - \tilde{\mathbf{z}}_k) + (\rho/2)\|\mathbf{x}_k - \tilde{\mathbf{z}}_k\|_2^2) \tag{11}$$

where $\boldsymbol{\lambda}_k \in \mathbb{R}^{N_k}$ is the dual variables associated with the coupling equality constraint, $\rho \in \mathbb{R}$ is the Lagrangian step.

Algorithm 1: ADMM.

1 $n = 0$: initial $\mathbf{z}^0$ and $\boldsymbol{\lambda}^0$ are given
2 **repeat**
3 $\quad$ $\mathbf{x}$ update: $\mathbf{x}_k^{n+1} = \underset{\mathbf{x}_k}{\text{argmin}} L_\rho(\mathbf{x}_k, \mathbf{z}^n, \boldsymbol{\lambda}_k^n) =$
$\quad\quad$ $\underset{\mathbf{x}_k}{\text{argmin}}(f_k(\mathbf{x}_k) + \boldsymbol{\lambda}_k^{nT}\mathbf{x}_k + (\rho/2)\|\mathbf{x}_k - \tilde{\mathbf{z}}_k^n\|_2^2)$
4 $\quad$ $\mathbf{z}$ update: $\mathbf{z}^{n+1} = \underset{\mathbf{z}}{\text{argmin}} L_\rho(\mathbf{x}_k^{n+1}, \mathbf{z}, \boldsymbol{\lambda}_k^n) =$
$\quad\quad$ $\underset{\mathbf{z}}{\text{argmin}} \sum_{k=1}^m (-\boldsymbol{\lambda}_k^{nT}\tilde{\mathbf{z}}_k + (\rho/2)\|\mathbf{x}_k^{n+1} - \tilde{\mathbf{z}}_k^n\|_2^2)$
5 $\quad$ $\boldsymbol{\lambda}$ update: $\boldsymbol{\lambda}^{n+1} = \boldsymbol{\lambda}_k^n + \rho(\mathbf{x}_k^{n+1} - \tilde{\mathbf{z}}_k^{n+1})$

The ADMM is summarized in Algorithm 1. The variables are alternatively updated in an iterative way. Although not shown directly in the mathematical formulation, at Step 4 of Algorithm 1, each component of the global variable can be determined by averaging all values of $\beta = x_k^{n+1} + (1/\rho)\lambda_k^n$ obtained via exchanging messages.

2) Distributed OPF: The OPF problem is formulated as:

$$\underset{\hat{\mathbf{v}}}{\text{minimize}}\ \hat{\mathbf{v}}^T \cdot \mathbf{z}^p \cdot \hat{\mathbf{v}} \tag{12}$$

$$\underset{\text{at } k=1,\cdots,N}{\text{subject to}} : P_k^{min} \le \hat{\mathbf{v}}_k^T \cdot \mathbf{z}_k^p \cdot \hat{\mathbf{v}}_k + P_k^L \le P_k^{max}, k \in \mathcal{G} \tag{13}$$

$$Q_k^{min} \le \hat{\mathbf{v}}_k^T \cdot \mathbf{z}_k^q \cdot \hat{\mathbf{v}}_k + Q_k^L \le Q_k^{max}, k \in \mathcal{G} \tag{14}$$

$$\hat{\mathbf{v}}_k^T \cdot \mathbf{z}_k^p \cdot \hat{\mathbf{v}}_k + P_k^L = 0, k \notin \mathcal{G} \tag{15}$$

$$\hat{\mathbf{v}}_k^T \cdot \mathbf{z}_k^q \cdot \hat{\mathbf{v}}_k + Q_k^L = 0, k \notin \mathcal{G} \tag{16}$$

$$(\mathbf{v}_k^{min})^2 \le (\mathbf{v}_k^{re})^2 + (v_k^{im})^2 \le (\mathbf{v}_k^{max})^2 \tag{17}$$

where $\hat{\mathbf{v}}$ is indicated by $\hat{\mathbf{v}} = \left[\mathbf{v}^{re}, \mathbf{v}^{im}\right]^T$; $\mathbf{v} = \mathbf{v}^{re} + \mathbf{v}^{im}$ is node voltage vector; P_{min}^k, P_{max}^k , Q_{min}^k, Q_{max}^k are active and reactive power limitation of generator at bus k; P_k^L, Q_k^L are load power at bus k; v_k^{min}, v_k^{max} are bus voltage thresholds.

Matrices $\mathbf{z}^p$ and $\mathbf{z}^q$ are obtained from:

$$\mathbf{z}^p = \begin{bmatrix} \mathbf{G} & -\mathbf{B} \\ \mathbf{B} & \mathbf{G} \end{bmatrix} \qquad \mathbf{z}^q = \begin{bmatrix} \mathbf{-B} & \mathbf{-G} \\ \mathbf{G} & \mathbf{-B} \end{bmatrix}$$

where $\mathbf{Y} = \mathbf{G} + j\mathbf{B}$ is the admittance matrix. $\mathbf{z}_k^p$ and $\mathbf{z}_k^q$ are the matrices with the sizes as $\mathbf{z}^p$ and $\mathbf{z}^q$ respectively, obtained by rewriting constraints in the quadratic form.

In order to solve the OPF problem in a distributed way, we need to split the problem (II-C2) into subsystems. The number of the subsystems corresponds to the number of buses in the network. The total active power losses can be expressed by decomposing the function into N parts:

$$\hat{\mathbf{v}}^T \cdot \mathbf{z}^p \cdot \hat{\mathbf{v}} = \sum_{k=1}^{N} \hat{\mathbf{v}}_k^T \cdot \mathbf{z}_k^p \cdot \hat{\mathbf{v}}_k \tag{18}$$

where $\hat{\mathbf{v}}_k$ is the vector having same size with $\hat{\mathbf{v}}$ and determined by replacing all elements not involved in bus k by zeros.

The subproblem at bus k involves in N_k buses and can be expressed as follows.

- If $k \notin \mathcal{G}$:

$$\begin{aligned} \underset{\hat{\mathbf{v}}_k}{\text{minimize}} \quad & \hat{\mathbf{v}}_k^T \cdot \mathbf{z}_k^p \cdot \hat{\mathbf{v}}_k \\ \text{subject to} \quad & (15), (16), (17) \end{aligned}$$

- If $k \in \mathcal{G}$:

$$\begin{aligned} \underset{\hat{\mathbf{v}}_k}{\text{minimize}} \quad & \hat{\mathbf{v}}_k^T \cdot \mathbf{z}^p \cdot \hat{\mathbf{v}}_k \\ \text{subject to} \quad & (13), (14), (17) \end{aligned}$$

where $\hat{\mathbf{v}}_k \in \mathbb{R}^{2N_k}$ is the local variable.

Note that variables of a subproblem are a set of voltages of local bus and adjacent buses. The OPF problem is therefore formulated in the general consensus problem as presented in (10) with additional equality and inequality constraints . The coupling constraint is: $\hat{\mathbf{v}}_k - \tilde{\mathbf{v}}_k = 0$, where $\tilde{\mathbf{v}}_k \in \mathbb{R}^{2N_k}$ is the global variable representing the collection of the related components of $\hat{\mathbf{v}} \in \mathbb{R}^{2N}$ that map into subsystem k.

III. The Multi-agent System

In this section, we present the agent-based system to deploy the proposed control in a cyber-physical MG. The MAS is a cluster of agents operated in a communication network. For the practical realization in realistic conditions, an agent has to be designed as an independent entity owning capabilities of receiving measurement from the device, communicating with other agents, processing calculations and then returning proper signals to the lower level controllers and actuators. The agents in this work will run two parallel processes corresponding to two control algorithms: the consensus algorithm in the SC and ADMM algorithm in the TC. As the real-world operation, the agents need to implement asynchronously under a real communication network to transfer data for consensus steps. The two control processes therefore need to be coordinated and expressed in detail for the real implementation. In the distributed scheme, instead of collecting all data to a central entity, each agent needs only local and adjacent information but could return system level signals to achieve global objectives. In this work, the neighborhood agents are defined based on electrical connections in the grid.

Remark 2: The communication network of MAS corresponds to the information connections in the distributed TC. However, the network is different from information connections in the distributed SC. MAS has to consider this issue for a proper implementation which covers both control levels.

A. Agent

Intuitively, each agent updates the state of the power network, processes the calculation and then returns control decisions. We classify agents into two main types of gen-agents and load-agents. Gen-agents are located at DG buses to send set-points to local controllers. Meanwhile, load-agents are put at load buses and join to the distributed control process, but will not return any control signals.

Fig. 1 shows the control scheme for a DG with a local controller and the corresponding agent. The local controller is the PC which implements the droop control using only local measurements. To achieve the SC and TC objectives simultaneously, the agent contains two separate processes running in parallel: secondary process and tertiary process.

Remark 3: These two processes operate continuously. The tertiary process obtains local active and reactive power and sends the set-point outputs P^{Ter} to the secondary process.

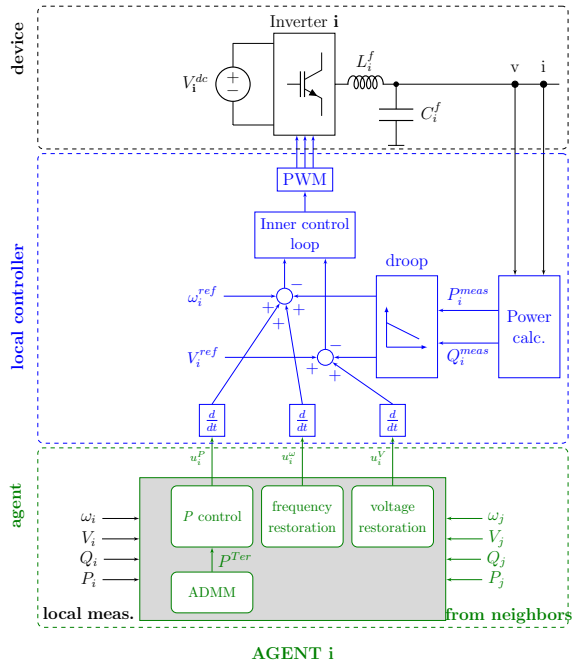

Fig. 1: Control diagram for a DG.

Concurrently, the secondary process receives voltage, frequency, active power from local measurement and P^{Ter} from the tertiary process to distribute control signals to the primary control. The two processes perform their tasks independently and the P^{Ter} message is exchanged via a common memory. Fig. 3 clarifies the operation of a gen-agent. Due to the fact that the ADMM calculation in the tertiary process much slower than the secondary response speed, P^{Ter} received by the secondary process will be held until a new one is updated from the tertiary process. The initial P^{Ter} value is set to zero.

B. Secondary Process

As presented in Section II.B, the communication considered in the distributed SC is based on the connections between DG buses. It means that agents at all nodes of the communication graph belong to gen-agent type as illustrated in Fig. 2a. However, the network for the agent system in this proposed framework consists of all buses of the grid and gen-agents are dispersed in the network as shown in Fig. 2b. Agents process a mechanism to deploy the distributed consensus control under the provided communication network.

From the consensus laws (7-9), a gen-agent should have knowledge of at least one other gen-agent to implement the calculation. After an iteration of exchanging data, agents only have information of its neighbors. Thus, in some cases, one gent-agent could not collect data of any other gen-agents for the consensus calculation. In order to overcome this challenge, we propose a solution that: instead of broadcasting local information in one single iteration, each agent processes several intermediate iterations for collecting and distributing data before computing the control laws. So instead of moving only on one edge, the local information will be sent on several edges in the network graph. A consensus loop is defined as

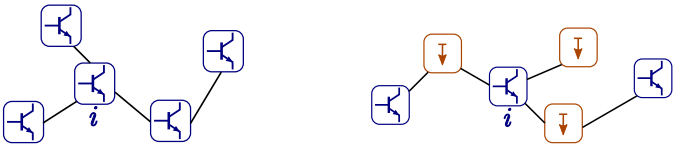

(a) Communication graph based on DG buses

(b) Communication graph in the proposed network

Fig. 2: Two kinds of communication graph

Algorithm 2: The secondary process in Agent k.

1 $I = 1$ // begin a loop at initial iteration
2 $\mathcal{N}^k \leftarrow \mathcal{N}_0^k$ // list of neighborhood agents
3 $\omega_k, V_k, K_k^P(P_k - P_k^{Ter})$ // obtain local measurement at node k
4 **while** $I < I_0^{cons}$ **do**
5 Distribute the local measurement to all neighbors
6 Collect from all neighbors $\omega_j, V_j, K_j^P(P_j - P_j^{Ter})$
7 $I = I + 1$ // move to the next iteration
8 Calculate control signals u_k^P, u_k^ω, u_k^V based on local information and neighborhood information // control laws (7), (8), (9)
9 Send the control values to the corresponding local controller // finish the current loop
10 **redo** from step 1 // start a new loop

the duration from the iteration when the agent receives local measurements to the iteration when the agent sends control signals. The purpose is that gen-agents can absorb information from at least another one.

Some denotations are given as follows. The distance between two gen-agents d_{ij} is the smallest number of edges in the network topology to go from agent i to agent j; the number of transferring iterations needed for gent-agent i can exchange data with at least one other gen-agent is $I_i^{min} = \min\{d_{ij}, \forall j \in \mathcal{G}, j \neq i\}$. The total number of iterations I_0^{cons} in a consensus loop will be set to a same value to all agents as:

$$I_0^{cons} = max\{I_i^{min}, \forall i \in \mathcal{G}\} \tag{19}$$

Agent j is a neighbor of agent i if $I_i^{min} \leq d_{ij} \leq I_0^{cons}$. Agents conduct consensus loops consecutively for the SC objectives. In one loop, the actual calculations of the consensus laws only happen at the iteration $I_0^{cons}th$. The remain iterations are for transferring local measurements among gen-agents. The agents only need I_0^{cons} values when the MAS is started. When the grid structure has any changes such as shutting down a DG, the agents may have installed mechanisms to on-line adapt to the changes.

In the MAS operation, load-gents only consist of iterations for transferring data. Meanwhile, gen-agents include iterations for sending signals to local controllers. Algorithm 2 describes the iterative algorithm for the secondary process in a consensus loop. Initially, agents collect local measurement $\{\omega_k, V_k, P_k\}$ from devices and exchange message $\{\omega_k, V_k, K_k^P(P_k - P_k^{Ter})\}$ among neighbors. Control signals will be computed and sent to controllers when a loop is finished. The reference frequency is

Algorithm 3: The tertiary process in Agent k.

1 $I = 1$ // begin a loop at initial iteration
2 $\mathbf{N}_k$ // list of neighborhood agents
3 P_k^L, Q_k^L // initial state, active and reactive power of load measured locally at node k
4 $\tilde{\mathbf{v}}_k(I) \leftarrow \tilde{\mathbf{v}}_0$ // initial global variables
5 $\boldsymbol{\lambda}_k(I) \leftarrow \boldsymbol{\lambda}_0$ // initial Lagrangian multipliers
6 **while** $I < I_0^{admm}$ **do**
7 Solve the local non-convex optimization problem to update the local variables $\mathbf{v}_k(I+1)$. Note that with the DG buses, the local voltage is set to a reference value. The problem at this bus is:

$$\underset{\hat{\mathbf{v}}_k}{\text{minimize}} \quad \hat{\mathbf{v}}_k^T \cdot \mathbf{z}^p \cdot \hat{\mathbf{v}}_k + \boldsymbol{\lambda}_k^T(I)\mathbf{v}_k + (\rho/2)\|\hat{\mathbf{v}}_k - \tilde{\mathbf{v}}_k(I)\|_2^2$$

$$\text{subject to} \quad (13), (14)$$

$$(v_k^{re})^2 + (v_k^{im})^2 = v_{ref}^2$$

$$(v_j^{min})^2 \le (v_j^{re})^2 + (v_j^{im})^2 \le (v_j^{max})^2, \quad \forall j | ((k,j) \in \mathcal{V}, j \ne k)$$

8 $\mathbf{B}_k(I+1) = \hat{\mathbf{v}}_k(I+1) + \frac{1}{\rho}\boldsymbol{\lambda}_k(I)$
9 Distribute $\mathbf{B}$ to all neighbors
10 Collect $\mathbf{B}$ from all neighbors
11 Averaging all $\mathbf{B}$ to update $\tilde{\mathbf{v}}_k(I+1)$
12 Update Lagrangian multiplier: $\boldsymbol{\lambda}_k(I+1) = \boldsymbol{\lambda}_k(I) + \rho(\hat{\mathbf{v}}_k(I+1) - \tilde{\mathbf{v}}_k(I+1))$
13 $I = I + 1$ // move to the next iteration
14 If agent k is the gen-agent, computing the set-point power outputs for the corresponding DG:

$$P_k^{Ter} = \hat{\mathbf{v}}_k^T \cdot \mathbf{z}_k^p \cdot \hat{\mathbf{v}}_k + P_k^L$$

15 Send P_k^{Ter} to the secondary process // finish the current loop
16 **redo** from step 1 // start a new loop

adjusted by the signals u_k^ω and u_k^P; while the reference voltage is adjusted by the signal u_k^V. Although several iterations are added in a consensus loop compared with other methods, the speed of updating signals to controllers is still fast because there are only forward messages processes or simple calculation processes in each iteration. This can satisfy the short timescale requirement for the SC.

C. Tertiary Process

This process runs the ADMM algorithm. The measurement inputs are active and reactive power of local load $\{P_k^L, Q_k^L\}$ and the messages exchanged with neighbors within an iteration transferred via the same channels used by the secondary process. The implementation of this process is presented in Algorithm 3. Considering gen-agents, the optimal result when finishing an ADMM loop, which is the reference active power, will be sent to the secondary process to update the active power reference P_k^{Ter} in the active power control law as shown in (9). In Step 7 of the Algorithm, an equality voltage constraint is inserted because the SC always keeps the voltage of DG terminal at a reference value.

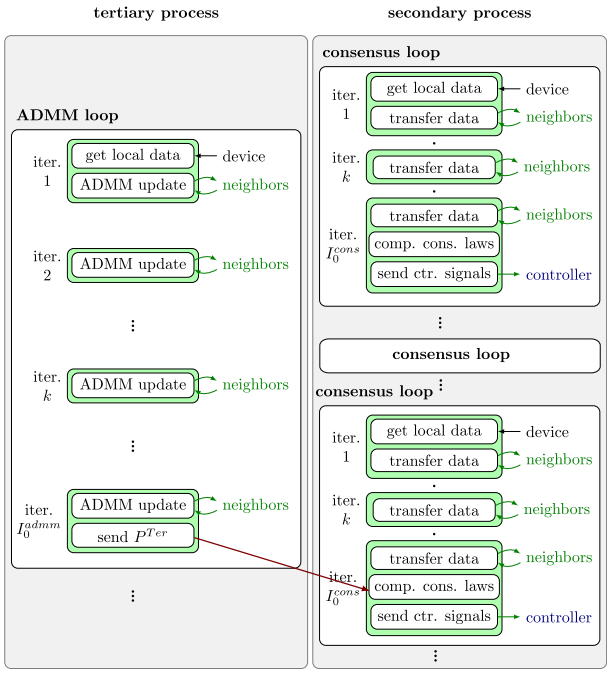

Fig. 3: The two iterative processes in a gen-agent.

Agents execute the loops consecutively to always seek the optimal points for DGs outputs. A ADMM loop is begun from iteration 1 when the agent receives measurements and finished at iteration I_0^{admm} when reaching the consensus. At the very first iteration, the agents do not know about system states. In this case, the initial guess of the global variables in each agent is set as $\mathbf{v}_k^{re}(0) = \mathbf{v}^{max}, \mathbf{v}_k^{im}(0) = \mathbf{0}$, the initial guess of the Lagrangian multipliers is set to zeros $\boldsymbol{\lambda}_0^k = \mathbf{0}$. Then, from the second ADMM loop, the starting points of the global variables and the Lagrangian multipliers are the solutions of the previous ADMM loop. In other words, the starting point is the current state of the system.

IV. The Real-time Cyber-Physical Setup and Experimental Results

A. Test Case MG and Cyber-Physical System Laboratory

This section presents the validation of the designed agents with the proposed distributed hierarchical control. We consider a six-bus islanded MG. The test case MG is controlled by three parallel DGs which corresponds to three local controllers. Loads are located at the remain buses. A laboratory of cyber-physical MG system has been setup including two main parts as shown in Fig. 4 and described as following.

1) Physical system: The physical system covers electrical MG elements and local controllers that are simulated to run in a real-time simulator OPAL-RT. The grid parameters and the secondary controllers are shown in Table I and II respectively.

2) Cyber system: The cyber system constitutes the hardware MAS and the communication network. An agent is a program written by python program language. Each agent is run independently in a Raspberry PI with a physical communication system. The communication topology is identical to the electrical grid network.

TABLE I: Parameters of the MG test case.

Line	Impedance (pu)	Reference
1-4	1.875+j1.228	$V_{ref} = 230V$
1-5	1.156+j0.491	
2-4	1.344+j0.969	$f_{ref} = 50Hz$
2-5	0.781+j2.469	
3-5	1.625+j1.063	$S_{ref} = 100kWA$
3-6	1.875+j1.228	

TABLE II: Parameters of secondary controllers.

	DG1	DG2	DG6
Droop controller	$K_1^P = 2e-4$ $K_1^Q = 2e-6$	$K_2^P = 2e-4$ $K_2^Q = 2e-6$	$K_6^P = 1.5e-4$ $K_6^Q = 1.5e-6$
Frequency controller	$c_1^1 = 0.1$	$c_1^2 = 0.1$	$c_1^3 = 0.1$
Voltage controller	$c_2^1 = 0.1$	$c_2^2 = 0.1$	$c_2^6 = 0.1$
Power sharing controller	$c_3^1 = 0.1$	$c_3^2 = 0.1$	$c_3^6 = 0.1$

Remark 4: With this test-bench design, the MAS can be proven the ability of operating in realistic conditions. The hardware agents run asynchronously with the measurements from the physical system. Each agent is a device with a specific IP address and the information is exchanged among agents via the real communication network. The agents consume time to handle the proposed distributed algorithm and to transfer data before returning the results to the local controllers, that reflect the real-world operation.

B. Experimental Results

1) Case 1: Validation under step response: In Case 1, the proposed control system is verified with step load changes. The studied MG is simulated to run in 700s with the load profiles shown in Fig. 5. We investigate the operation of the proposed framework by collecting recording data from two sources: one is the logging files of the agents for checking the calculation in each iteration, and one is the measurement data saved in the simulator for observing system operation.

There are five milestones in Fig. 6 we need to take into account: t_2 and t_4 when the disturbances occur in the system due to the changing of load power; t_1, t_3 and t_5 when the agents complete an ADMM loop and update new P^{Ter} to the local controllers.

When a disturbance occurs in the system, specifically a load step change, the objectives will be:

- In the SC level which has the response speed in seconds: the system frequency is restored to the nominal value of $50Hz$; the voltages at DG buses are kept at $1.05pu$, while the voltages at remain buses are guaranteed in $[0.9, 1.1]$, which is the range between lower and upper voltage thresholds; the active power outputs generated by DGs are shared proportionally following the energy capacity.
- In the TC level which has a slower dynamic response: the power outputs of DGs are redistributed to reduce total power losses to a minimal value. The results will be compared with the results solved by the centralized approach to show the precision of the method.

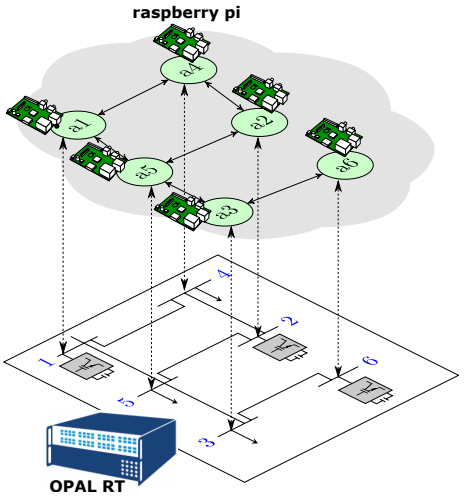

Fig. 4: The test case MG in the layer structure.

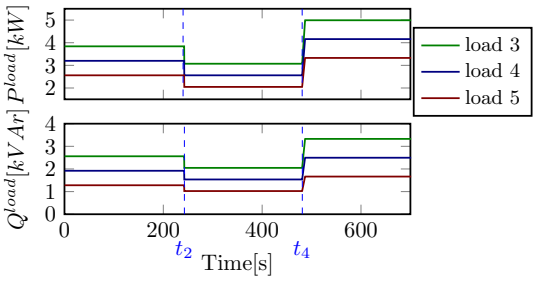

Fig. 5: Active and reactive power of loads.

Firstly, the achievement of the SC objectives is confirmed by considering the performance of frequency f^{meas}, voltage V^{meas} and active power P^{meas} sensed at DG outputs. The computation in the ADMM process of the corresponding agents in the same time frame is also regarded. The active power output of DG computed by agent is denoted as P^{comp}. In this section, we only analyze the measurements of the system at DG 1 as demonstrated in Fig. 6. The three DGs operate in parallel and have the same control structure. The results at DG 2 and DG 6 therefore can be studied in a similar way. From the logging files of the agents, we can observe that the ADMM process in each agent runs 12 ADMM loops from l_1 to l_{12}, one loop consists of 1000 iterations. We now investigate important milestones as follows.

The MG with the MAS is started at $t = 0s$. The secondary process in the agent running the consensus algorithm to update the voltage and frequency reference in the inverter controller. The bus voltage and frequency are regulated to move to nominal values gradually. Concurrently, in agent 1, the tertiary process executes the first ADMM loop when it gets the measurement inputs at $0s$ and finishes the loop at $t_1 = 56.8s$. The computation for the optimal set-point active power of DG 1 in the loop l_1 is clarified by zooming out as shown in the sub-figure on the top. In this period, the agent coordinates to the neighbors and proceed 1000 iterations of ADMM. We can see the convergence of the computation is affirmed when

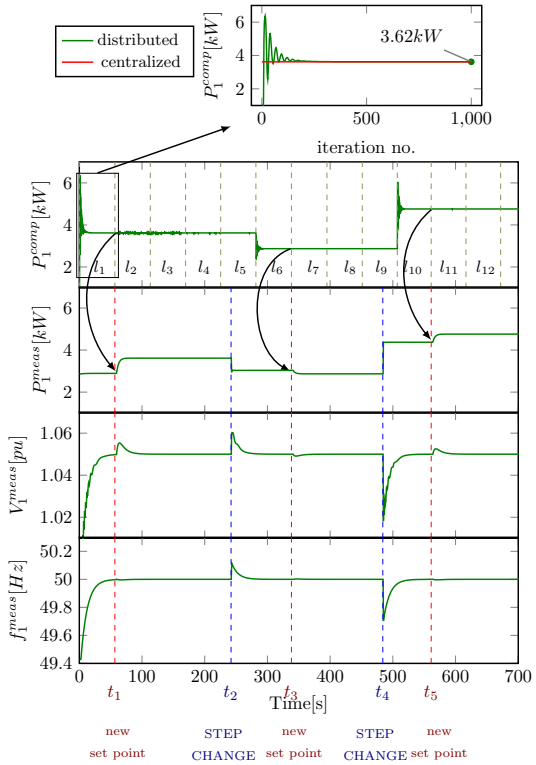

Fig. 6: The convergence of active power calculation in agent 1 and the measurements at bus 1.

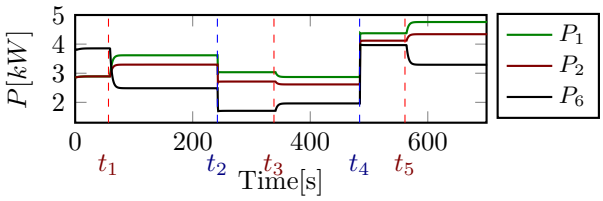

Fig. 7: The active power outputs of the DGs.

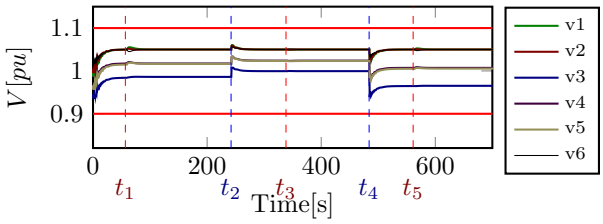

Fig. 8: The bus voltages.

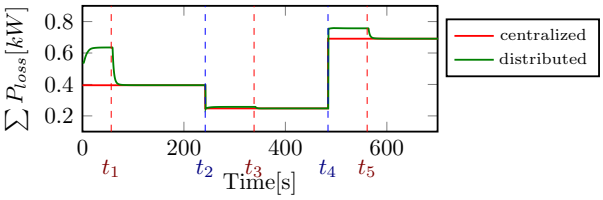

Fig. 9: The total active power losses of the network.

comparing with the result obtained in the centralized approach.

At the $1000th$ iteration of l_1 or at t_1, P^{Ter} value in the calculation of the secondary process is updated. The active power produced by DG 1 is then followed the optimal value found out in the tertiary process. In the following loop from l_2 to l_5, the active power calculated in each iteration is nearly unchanged since the MG already reached the steady state.

At $t_2 = 240s$, the load burden is decreased. The frequency and bus voltage suffer a sudden rise, but they can rapidly be restored to the references in time thanks to the activation of the secondary process in the agent. The tertiary process, at the beginning of the ADMM loop l_6, recognizes the system variation and sends the new set-point at the end of the loop $t_3 = 338s$ to make the DG operates at the new optimal state. A similar process happens at $t_4 = 480s$ when the loads are made an increased step.

The power sharing between DGs is presented in more detail in Fig. 7. When occurring load variations, first the power outputs of DGs still follow ADMM results. Then the power mismatch between suppliers and consumers will be shared by SC proportionally. Therefore, in periods the ADMM processes are not completed to respond to new operation states of the system, specifically $0-t_1$, t_2-t_3 and t_4-t_5, the DGs generate active power following the droop coefficients with power references are outputs of the previous ADMM loop. Notably, at the beginning from $0s$ to $t_1 s$ when P^{Ter} is set to zero for all inverter controllers, we can see obviously that the active power measured at bus 1 equal to at bus 2 due to the analogy of the associated droop coefficients. In the remain duration, the power outputs are controlled arbitrarily complying with the consequences of the distributed OPF process.

Fig. 8 shows bus voltages. The voltages at DG buses are always recovered and maintained at $1.05pu$. Meanwhile, the voltages at load buses are varied within allowable limits of $[0.9, 1.1]$. The upper and lower thresholds are represented by thick red lines in the figure. The total active power losses of the network are calculated and presented in Fig. 9. In the same load condition, the value of $\sum P^{loss}$ is always declined which saving the operating cost of the system. The power loss achieved by the designed framework is identical to the loss when solving the OPF problem in a centralized way.

Finally, we investigate the agreement between the mathematical computation in the agents and the measurements from the simulation. Fig. 10 shows the convergence of DG reactive power in the ADMM calculation in the gen-agents, and the measured reactive power collected from the simulator. It is worth noting that in the proposed control framework the agents do not deliver the reactive power references to the lower control level. The inverter controllers regulate only active power outputs and bus voltages of DGs. However, the DGs can provide power values, both active and reactive, which are tracked to the references calculated by the agents.

2) Case 2: Adding communication delay: In case 2, the performance of the proposed platform is validated under emulated communication network. In case 1, as shown in Fig. 4, the RPIs (or agents) are connected to the same laboratory Ethernet network. Although the real network is used, it may not reflect correctly what happens in practical applications with long distances between agents and different communication technologies.

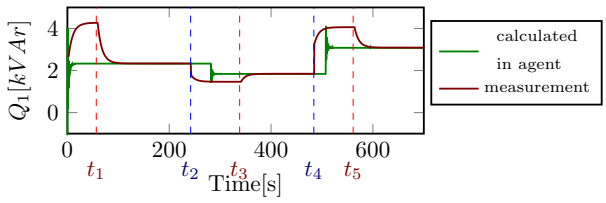

Fig. 10: The reactive power outputs of the DGs from agent calculation and from simulation measurements at bus 1.

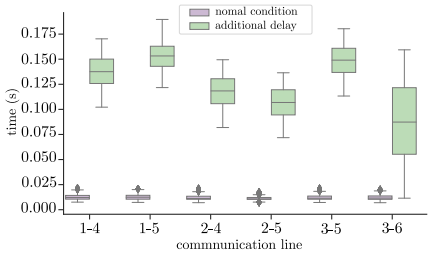

Fig. 11: Latency measurement in normal condition network and in additional delay network.

The network emulation is conducted based on the traffic control utility (TC) and NetEm, and it was inspired by the work in [29]. The data transfer time in emulated network is measured and illustrated in Fig. 11 in comparison with normal condition network. It can be seen that different communication lines have different latency ranges.

A similar study with load step changes is deployed to investigate the operation of the grid with the proposed control under the new communication network environment. The measurements of bus voltages, frequency and total power losses are presented in Fig. 12. The duration of the test is prolonged because, with larger latencies, the agents need more time to complete ADMM calculations. As shown in the figure, the voltages at DG buses and system frequency are always recovered at reference values after disturbances. Furthermore, the grid operation achieves the optimal state as the fact that the collected total power losses of the network is identical to the value computed in the centralized way. Therefore, the hierarchical distributed control framework can tolerate communication network with higher time delays.

3) Case 3: Plug-and-play capability: In case 3, we check the plug-and-play capability of the designed agent system. The performance of the studied grid is illustrated in Fig. 13. Generator 6 is switched off manually at $t_1 = 135s$ following by the disconnection of agent 6 out of the multi-agent system. At this time, agent 5, which is agent 6's neighbor, reconfigures itself to adapt new network topology. Specifically, agent 5 removes agent 6 from its list of neighbors and updates values of z_p^k, z_q^k. The remain agents have no connection with agent 6, therefore they keep the parameters as before. As can be seen from the figure, the system with the five agents then operates correctly: bus voltages, frequency are restored and the power loss is minimized.

A load decreasing step is conducted at $t_2 = 220s$. After slight fluctuations, all control objectives of the system are achieved as shown in Fig. 13. The system therefore can work

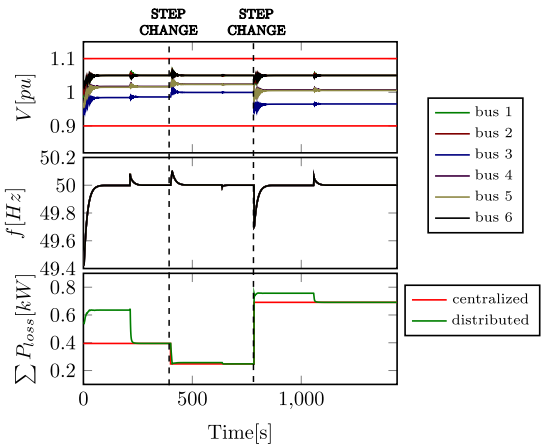

Fig. 12: The measured voltage, frequency and total power losses in Case 2.

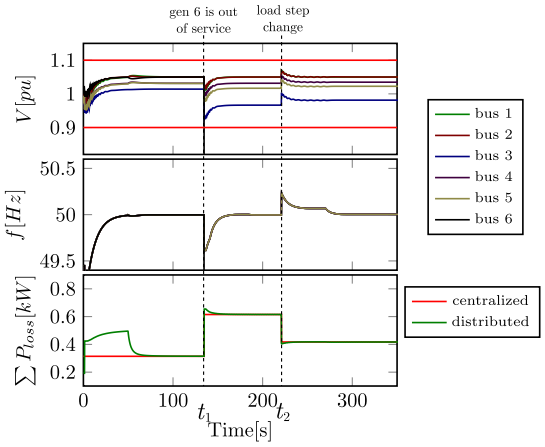

Fig. 13: The measured voltage, frequency and total power losses in Case 3.

appropriately without any interruption.

V. Conclusion

This paper presents a fully distributed hierarchical control scheme for islanded AC microgrids. Instead of using a central unit, a MAS is designed to operate in a sparse communication network. The agent-based control framework is built to obtain multiple objectives in different timescales. The agent with capabilities of computation and communication can simultaneously run two processes corresponding to two control levels. The secondary process implements the consensus algorithm to response quickly and achieves frequency restoration, voltage regulation as well as arbitrary active power sharing. Meanwhile, the tertiary process, in a slower response, uses ADMM to minimize the total power losses. The proposed control scheme only requires peer-to-peer communications, so the cyber resilience of the microgrid is enhanced.

The six-bus three-DG microgrid test system and the proposed control scheme has been developed in a cyber-physical microgrid platform for a practical validation. The results prove that the agents can work effectively and collaboratively to achieve the control objectives for MGs in an environment close to working conditions.

Future works will focus on two aspects: (i) the applications of the agent system covering multiple control level on another system, e.g. microgrid cluster system, hybrid AC/DC network system; and (ii) improving the cyber-physical platform by integrating hardware inverters into the real-time grid simulation.

APPENDIX

The closed-loop system is derived to analyze the system stability. The detailed process is as follow.

Let $\Delta\omega = \omega - \omega^*$ and $\Delta V = V - V^*$.$\Delta\theta$ is the power angle. The controllable units are $1, .., N$. From (5)-(6), it can be derived that

$$\Delta\dot{\theta} = \Delta\omega \tag{20}$$

$$\Delta\dot{\omega} = -\frac{1}{\tau^P}\Delta\omega - \frac{1}{\tau^P}K^P\Delta P + \frac{1}{\tau^P}\Delta\Omega \tag{21}$$

$$\Delta\dot{V} = -\frac{1}{\tau^Q}\Delta V - \frac{1}{\tau^Q}K^Q\Delta Q + \frac{1}{\tau^Q}\Delta\lambda \tag{22}$$

where $\Delta\theta = [\Delta\theta_1, ...\Delta\theta_N]^T$, $\Delta\omega = [\Delta\omega_1, ...\Delta\omega_N]^T$, $\Delta V = [\Delta V_1, ...\Delta V_N]^T$. τ^P, τ^Q, K^P, and K^Q are diagonal matrix. I is the Identity matrix.

Eq. (20)-(22) can be written in state-space form, as follows:

$$\begin{aligned}\left[\Delta\dot{\theta}, \Delta\dot{\omega}, \Delta\dot{V}\right]^T &= A_1\left[\Delta\theta, \Delta\omega, \Delta V\right]^T + B_1\left[\Delta P, \Delta Q\right]^T \\ &+ C_1\Delta\Omega + D_1\Delta\lambda\end{aligned} \tag{23}$$

where

$$A_1 = \begin{bmatrix}0 & I & 0\\ 0 & -\frac{1}{\tau^P} & 0\\ 0 & 0 & -\frac{1}{\tau^Q}\end{bmatrix}, B_1 = \begin{bmatrix}0 & 0\\ -\frac{1}{\tau^P}K^P & 0\\ 0 & -\frac{1}{\tau^Q}K^Q\end{bmatrix},$$
$$C_1 = \left[0, \tfrac{1}{\tau^P}, 0\right]^T, D_1 = \left[0, 0, \tfrac{1}{\tau^Q}\right]^T.$$

The secondary controllers designed in this paper can be rewritten in matrix form as:

$$\dot{\Omega} = -c_1 L\omega + c_1 G(\omega^*\mathbf{1} - \omega) - c_3 L(K^P P - P^{Ter}) \tag{24}$$

$$\dot{\lambda} = -c_3 LV + c_3 G(V^*\mathbf{1} - V) \tag{25}$$

where $\Omega, \omega, P, P^{Ter}, \omega, V, \mathbf{1}$ are vectors with $N\times 1$ dimension. L, G, K^P are matrices with $N \times N$ dimension, and $K^P = diag\{K_1^P, ..., K_N^P\}$.

In small-signal form, (24) and (25) can be rewritten as

$$\Delta\dot{\Omega} = A_2\Delta\omega + B_2\Delta P + C_2 \tag{26}$$

where $A_2 = -c_1(L+G), B_2 = -c_3 LK^P, C_2 = c_1 G\omega^*\mathbf{1} + c_3 LP^{Ter}$.

$$\Delta\dot{\lambda} = A_3\Delta V + B_3 \tag{27}$$

where $A_3 = -c_2(L+G), B_3 = c_2 GV^*\mathbf{1}$.

Combining the SC (26) and (27) into the state-space model in (23)

$$\begin{aligned}\left[\Delta\dot{\theta}, \Delta\dot{\omega}, \Delta\dot{V}, \Delta\dot{\Omega}, \Delta\dot{\lambda}\right]^T &= A_4\left[\Delta\theta, \Delta\omega, \Delta V, \Delta\Omega, \Delta\lambda\right]^T \\ &= B_4\left[\Delta P, \Delta Q\right]^T + C_4\end{aligned} \tag{28}$$

where

$$A_4 = \begin{bmatrix}0 & I & 0 & 0 & 0\\ 0 & -\frac{1}{\tau^P} & 0 & \frac{1}{\tau^P} & 0\\ 0 & 0 & -\frac{1}{\tau^Q} & 0 & \frac{1}{\tau^Q}\\ 0 & A_2 & 0 & 0 & 0\\ 0 & 0 & A_3 & 0 & 0\end{bmatrix}, B_4 = \begin{bmatrix}0 & 0\\ -\frac{K^P}{\tau^P} & 0\\ 0 & -\frac{K^Q}{\tau^Q}\\ B_2 & 0\\ 0 & 0\end{bmatrix},$$
$$C_4 = \left[0, 0, 0, C_2, C_3\right]^T.$$

Furthermore, considering the power network model as:

$$\begin{bmatrix}\Delta P\\ \Delta Q\end{bmatrix} = \begin{bmatrix}B & G\\ -G & B\end{bmatrix}\begin{bmatrix}\Delta\theta\\ \Delta V\end{bmatrix} = \Gamma\begin{bmatrix}\Delta\theta\\ \Delta V\end{bmatrix} \tag{29}$$

Substituting (29) into (28), it obtains:

$$\begin{aligned}&\left[\Delta\dot{\theta}, \Delta\dot{\omega}, \Delta\dot{V}, \Delta\dot{\Omega}, \Delta\dot{\lambda}\right]^T \\ &= A_4\left[\Delta\theta, \Delta\omega, \Delta V, \Delta\Omega, \Delta\lambda\right]^T + B_4\Gamma\left[\Delta\theta, \Delta V,\right]^T + C_4 \\ &= (A_4 + B_4\Gamma T)\left[\Delta\theta, \Delta\omega, \Delta V, \Delta\Omega, \Delta\lambda\right]^T + C_4\end{aligned} \tag{30}$$

where $T = \begin{bmatrix}I & 0 & 0 & 0 & 0\\ 0 & 0 & I & 0 & 0\end{bmatrix}$.

Therefore, the system state-space model $\dot{x} = A_{sys}x$ is derived. To ensure system stability, the control gains should be selected that the eigenvalues of the system matrix A_{sys} are located at the Left Half plane.

REFERENCES

[1] N. Hatziargyriou, *Microgrids: Architectures and Control*. Wiley, 2014.

[2] D. E. Olivares et al., "Trends in microgrid control," *IEEE Transactions on Smart Grid*, vol. 5, no. 4, pp. 1905–1919, 2014.

[3] S. K. Sahoo, A. K. Sinha, and N. K. Kishore, "Control techniques in ac, dc, and hybrid ac–dc microgrid: A review," *IEEE Journal of Emerging and Selected Topics in Power Electronics*, vol. 6, no. 2, pp. 738–759, June 2018.

[4] J. M. Guerrero, M. Chandorkar, T. Lee, and P. C. Loh, "Advanced Control Architectures for Intelligent Microgrids; Part I: Decentralized and Hierarchical Control," *IEEE Transactions on Industrial Electronics*, vol. 60, no. 4, pp. 1254–1262, 2013.

[5] K. Yousef et al., "On the secondary control architectures of ac microgrids: An overview," *IEEE Transactions on Power Electronics*, 2020.

[6] J. W. Simpson-Porco, Q. Shafiee, F. Dörfler, J. C. Vasquez, J. M. Guerrero, and F. Bullo, "Secondary frequency and voltage control of islanded microgrids via distributed averaging," *IEEE Transactions on Industrial Electronics*, vol. 62, no. 11, pp. 7025–7038, Nov 2015.

[7] J. Liu, J. Li, H. Song, A. Nawaz, and Y. Qu, "Nonlinear secondary voltage control of islanded microgrid via distributed consistency," *IEEE Transactions on Energy Conversion*, pp. 1–1, 2020.

[8] Z. Zhao, J. Guo, C. S. Lai, H. Xiao, K. Zhou, and L. L. Lai, "Distributed model predictive control strategy for islands multi-microgrids based on non-cooperative game," *IEEE Transactions on Industrial Informatics*, pp. 1–1, 2020.

[9] G. Lou, W. Gu, J. Wang, W. Sheng, and L. Sun, "Optimal design for distributed secondary voltage control in islanded microgrids: Communication topology and controller," *IEEE Transactions on Power Systems*, vol. 34, no. 2, pp. 968–981, 2019.

[10] F. Guo, L. Wang, C. Wen, D. Zhang, and Q. Xu, "Distributed voltage restoration and current sharing control in islanded dc microgrid systems without continuous communication," *IEEE Transactions on Industrial Electronics*, vol. 67, no. 4, pp. 3043–3053, 2020.

[11] Y. Wang, T. L. Nguyen, Y. Xu, Z. Li, Q. T. Tran, and R. Caire, "Cyber-Physical Design and Implementation of Distributed Event-Triggered Secondary Control in Islanded Microgrids," *IEEE Transactions on Industry Applications*, vol. 55, no. 6, pp. 5631–5642, 2019.

[12] R. de Azevedo, M. H. Cintuglu, T. Ma, and O. A. Mohammed, "Multiagent-based optimal microgrid control using fully distributed diffusion strategy," *IEEE Transactions on Smart Grid*, vol. 8, no. 4, pp. 1997–2008, 2017.

[13] D. K. Molzahn, F. Dörfler, H. Sandberg, S. H. Low, S. Chakrabarti, R. Baldick, and J. Lavaei, "A survey of distributed optimization and control algorithms for electric power systems," *IEEE Transactions on Smart Grid*, vol. 8, no. 6, pp. 2941–2962, Nov 2017.

[14] Y. Wang, S. Wang, and L. Wu, "Distributed optimization approaches for emerging power systems operation: A review," *Electric Power Systems Research*, vol. 144, pp. 127–135, 2017.

[15] W. Lu, M. Liu, S. Lin, and L. Li, "Incremental-oriented admm for distributed optimal power flow with discrete variables in distribution networks," *IEEE Transactions on Smart Grid*, vol. 10, no. 6, pp. 6320–6331, 2019.

[16] S. Mhanna, G. Verbič, and A. C. Chapman, "Adaptive admm for distributed ac optimal power flow," *IEEE Transactions on Power Systems*, vol. 34, no. 3, pp. 2025–2035, 2019.

[17] A. Engelmann, Y. Jiang, B. Houska, and T. Faulwasser, "Decomposition of non-convex optimization via bi-level distributed aladin," *IEEE Transactions on Control of Network Systems*, pp. 1–1, 2020.

[18] G. Chen, F. L. Lewis, E. N. Feng, and Y. Song, "Distributed optimal active power control of multiple generation systems," *IEEE Transactions on Industrial Electronics*, vol. 62, no. 11, pp. 7079–7090, Nov 2015.

[19] Z. Li, Z. Cheng, J. Liang, J. Si, L. Dong, and S. Li, "Distributed event-triggered secondary control for economic dispatch and frequency restoration control of droop-controlled ac microgrids," *IEEE Transactions on Sustainable Energy*, vol. 11, no. 3, pp. 1938–1950, 2020.

[20] X. Wu, L. Chen, C. Shen, Y. Xu, J. He, and C. Fang, "Distributed optimal operation of hierarchically controlled microgrids," *IET Generation, Transmission Distribution*, vol. 12, no. 18, pp. 4142–4152, 2018.

[21] A. Bidram, F. L. Lewis, and A. Davoudi, "Distributed control systems for small-scale power networks: Using multiagent cooperative control theory," *IEEE Control Systems Magazine*, vol. 34, no. 6, pp. 56–77, Dec 2014.

[22] A. Mustafa, B. Poudel, A. Bidram, and H. Modares, "Detection and mitigation of data manipulation attacks in ac microgrids," *IEEE Transactions on Smart Grid*, vol. 11, no. 3, pp. 2588–2603, 2020.

[23] H. Almasalma, S. Claeys, K. Mikhaylov, J. Haapola, A. Pouttu, and G. Deconinck, "Experimental validation of peer-to-peer distributed voltage control system," *Energies*, vol. 11, no. 5, 2018. [Online]. Available: https://www.mdpi.com/1996-1073/11/5/1304

[24] M. J. Stanovich, S. K. Srivastava, D. A. Cartes, and T. L. Bevis, "Multi-agent testbed for emerging power systems," in *2013 IEEE Power Energy Society General Meeting*, July 2013, pp. 1–5.

[25] K. Khadedah, V. Lakshminarayanan, N. Cai, and J. Mitra, "Development of communication interface between power system and the multi-agents for micro-grid control," in *2015 North American Power Symposium (NAPS)*, Oct 2015, pp. 1–6.

[26] S. Zuo, A. Davoudi, Y. Song, and F. L. Lewis, "Distributed Finite-Time Voltage and Frequency Restoration in Islanded AC Microgrids," *IEEE Transactions on Industrial Electronics*, 2016.

[27] R. Olfati-Saber, J. A. Fax, and R. M. Murray, "Consensus and cooperation in networked multi-agent systems," *Proceedings of the IEEE*, vol. 95, no. 1, pp. 215–233, Jan 2007.

[28] J. E. S. Boyd, N. Parikh, E. Chu, B. Peleato, "Distributed Optimization and Statistical Learning via the Alternating Direction Method of Multipliers," *Foundations and Trends in Machine Learning*, 2011.

[29] C. Gavriluta, C. Boudinet, F. Kupzog, A. Gomez-Exposito, and R. Caire, "Cyber-physical framework for emulating distributed control systems in smart grids," *International Journal of Electrical Power & Energy Systems*, vol. 114, p. 105375, 2020.

Tung-Lam Nguyen received the Master's degree in electrical engineering from National Taiwan University of Science and Technology, Taiwan, in 2014, and the Ph.D. degree from the University of Grenoble Alpes, Grenoble, France, in 2019. He was a Post-Doctoral Researcher with the Grenoble Institute of Technology, Grenoble, France, as part of the G2ELab. He is currently a Lecturer with the Faculty of Electrical Engineering, University of Science and Technology, The University of Danang, Vietnam. His research interests include distributed control and optimization, interoperability and co-simulation in smart grid.

Yu Wang (S'12-M'17) received the B.Eng. degree in School of Electrical Engineering and Automation from Wuhan University, China in 2011, and the M.Sc. and Ph.D. degree in Power Engineering from Nanyang Technological University, Singapore in 2012 and 2017, respectively. He is currently a research fellow in Nanyang Technological University, Singapore. He leads industry projects on hybrid microgrid systems, energy storage systems, and cyber-security of power systems. His research interests include distributed control and optimization in electrical systems, microgrids and cyber-physical systems.

Quoc-Tuan Tran received his Ph.D. degree in Electrical Engineering from the Grenoble Institute of Technology in 1993. He is currently a Professor with INSTN – Paris Saclay University, and a Scientific Manager with Alternative Energies and Atomic Energy Commission (CEA) - National Institute for Solar Energy (INES). His research interests are in the fields of power system analysis, operations, electromagnetic transients, distributed generation, smart-grid and renewable energy. He is an IEEE senior member.

Raphael Caire received the Diplôme d'Etudes Approfondies and Doctorat de l'INPG degrees from the Institut National Polytechnique de Grenoble in 2000 and 2004, respectively. He is currently an Associate Professor with the Grenoble Institute of Technology, Ecole d'ingénieurs en énergie eau et environnement, Grenoble Electrical Engineering Laboratory. His research is centered on the impacts, production control of dispersed generation on distribution system and critical infrastructures. He is an IEEE senior member.

Yan Xu (S'10-M'13) received the B.E. and M.E degrees from South China University of Technology, Guangzhou, China in 2008 and 2011, respectively,and the Ph.D. degree from The University of Newcastle, Australia, in 2013. He is now the Nanyang Assistant Professor at School of Electrical and Electronic Engineering, Nanyang Technological University (NTU), and a Cluster Director at Energy Research Institute @ NTU (ERI@N), Singapore. Previously, he held The University of Sydney Post-doctoral Fellowship in Australia. His research interests include power system stability and control, microgrid, and data-analytics for smart grid applications. Dr Xu is an Editor for IEEE Transactions on Smart Grid, IEEE Transactions on Power Systems, IEEE Power Engineering Letters, CSEE Journal of Power and Energy Systems, and an Associate Editor for IET Generation, Transmission & Distribution.

Catalin Gavriluta received his M.Sc. degree in Wind Power Systems from Aalborg University, Aalborg, Denmark, in 2011 and his Ph.D. degree from the Technical University of Catalonia, Barcelona, Spain in 2015. Before joining AIT as a Research Engineer in November 2017, he was enrolled for two years as a post-doc researcher with the Grenoble Institute of Technology, Grenoble, France working as part of the G2ELab. His work and interests are oriented towards smart grids and microgrids, with specific focus on the control of distributed cyber-physical systems, as well as on the testing and validation of such systems using hardware and controller in the loop approaches.